AFRL-SR-BL-TR-00

0008

REPORT DOCUMENTATION PAGE

1. AGENCY USE ONLY (*Leave Blank*)

2. REPORT DATE
1/4/00

3. REPO[RT TYPE AND DATES COVERED]
Final Technical, 3/1/97 to 12/31/99

4. TITLE AND SUBTITLE
RAYLEIGH IMAGING OF MACH 8 BOUNDARY LAYER FLOW AROUND AN ELLIPTIC CONE BODY

5. FUNDING NUMBERS
PE -
PR -
SA -
G - F49620-97-1-0181

6. AUTHORS
Richard B. Miles and Alexander J. Smits

7. PERFORMING ORGANIZATION NAME(S) AND ADDRESS(ES)
Department of Mechanical & Aerospace Engineering, Princeton University
Princeton, NJ 08544

8. PERFORMING ORGANIZATION REPORT NUMBER

9. SPONSORING / MONITORING AGENCY NAME(S) AND ADDRESS(ES)
Air Force Office of Scientific Research/NA (AFOSR), attn. Dr. Stephen Walker
801 North Randolph Street
Room 732
Arlington, VA 22203-1977

10. SPONSORING / MONITORING AGENCY REPORT NUMBER

11. SUPPLEMENTARY NOTES
The views, opinions and/or findings contained in this report are those of the author(s) and should not be construed as an official Department of the Army position, policy or decision, unless so designated by other documentation.

12a. DISTRIBUTION / AVAILABILITY STATEMENT
Approved for public release; distribution unlimited

12b. DISTRIBUTION CODE

13. ABSTRACT (*Maximum 200 words*)

This report is the Final Technical Report on AFOSR Grant #F49620-97-1-0181. Work on this project has focused on three areas:

- Pulse-burst laser system upgrade.
- The development and characterization of CO2-enhanced Filtered Rayleigh Scattering.
- Transition studies on flat plates and elliptic cones at Mach 8.

The pulse-burst laser has been shown to be an effective illumination source for capturing high-speed boundary layer and high-speed shock wave/ boundary layer images. That laser system was upgraded in association with a DURIP equipment grant (#F49620-97-1-0373) in order to produce a high-power, fully integrated laser system that could be used in the Mach 8 facility for the study of the transition dynamics on the 4:1 elliptic cones. Visualizations have been made using single-, double- and multiple-shot Rayleigh scattering, and the key results are summarized in this report.

14. SUBJECT TERMS
Hypersonic flow, boundary layers, turbulence, transition, elliptic cones

15. NUMBER OF PAGES
15

16. PRICE CODE

17. SECURITY CLASSIFICATION OF REPORT
UNCLASSIFIED

18. SECURITY CLASSIFICATION OF THIS PAGE
UNCLASSIFIED

19. SECURITY CLASSIFICATION OF ABSTRACT
UNCLASSIFIED

20. LIMITATION OF ABSTRACT
UL

NSN 7540-01-280-5500

Standard Form 298 (Rev. 2-89)
Prescribed by ANSI Std. Z39-1
298-102

20000114 044

FINAL TECHNICAL REPORT

RAYLEIGH IMAGING OF MACH 8 BOUNDARY LAYER FLOW AROUND AN ELLIPTIC CONE BODY

AFOSR GRANT #F49620-97-1-0181

Richard B. Miles and Alexander J. Smits
Department of Mechanical & Aerospace Engineering
Princeton University

Abstract
This report is the Final Technical Report on AFOSR Grant #F49620-97-1-0181. Work on this project has focused on three areas:

- Pulse-burst laser system upgrade.
- The development and characterization of CO_2-enhanced Filtered Rayleigh Scattering.
- Transition studies on flat plates and elliptic cones at Mach 8.

The pulse-burst laser has been shown to be an effective illumination source for capturing high-speed boundary layer and high-speed shock wave/ boundary layer images. That laser system was upgraded in association with a DURIP equipment grant (#F49620-97-1-0373) in order to produce a high-power, fully integrated laser system that could be used in the Mach 8 facility for the study of the transition dynamics on the 4:1 elliptic cones. Visualizations have been made using single-, double- and multiple-shot Rayleigh scattering, and the key results are summarized in this report.

Measurement Techniques
In order to address a general need for high speed imaging diagnostics, we have developed the capability of generating a "train" of on the order of 30-40 high energy pulses, separated in time by a variable period as short as one microsecond. The burst sequence is exceedingly flexible in both individual pulse duration and interpulse spacing, and can be repeated at repetition rates of 10 Hz (see Fig. 1).

An additional critical feature of the pulse-burst laser system is that the use of a single frequency master oscillator results in an exceedingly narrow (order 10's of MHz) and <u>tunable</u>, spectral output, therefore permitting Filtered Rayleigh Scattering (FRS) imaging (Lempert, et. al, 1997). The FRS technique utilizes a sharp cut-off atomic or molecular vapor filter to attenuate stray elastic scattering from model surfaces, while transmitting flow scattering. As illustrated in Fig. 2, when narrow bandwidth laser radiation is incident upon a flow field, elastically scattered light is superimposed upon the Doppler-shifted scattered light. If the laser is tuned to coincide with an absorption band of an optically thick vapor, and, if a cell filled with this vapor is placed in front of a detector, then the elastically scattered light will be strongly attenuated. In a Mach 8 flow, the Doppler shift is approximately 2.5 GHz, which is much greater than the approximately 0.3 GHz cut-off edge of an iodine vapor filter (Miles, et al., 1992). Therefore, by properly choosing the laser frequency with respect to the filter edge, the Doppler-shifted flow field scattering is essentially completely transmitted, whereas scattering interference from model surfaces is attenuated by orders of magnitude.

Measurements were done with a laser sheet and analyzed in two dimensions using a Nd:YAG laser. The laser is frequency-doubled to 532 nm and tuned to overlap a strong iodine vapor absorption line. This enables the use of a iodine vapor filter for filtered Rayleigh scattering. Iodine vapor is an almost ideal material for the filter and is particularly effective in suppressing background scattering from windows and walls. Suppression of the background scattering is very important since measurements must be made near the wall.

This technique has been effectively used in the Princeton Gas Dynamics Laboratory Mach 8 facility (Figure 3) in obtaining multiple-plane visualizations of the three-dimensional transition process on a 4:1 ellipsoidal cone. The pulse-burst technique has also been used to obtain many short "movies" of the flow development, typically with time steps of 2 microseconds. An example of the flow through a shock-wave boundary-layer interaction at Mach 2.5 is shown in Figure 4. The results for the Mach 8 elliptic cone flow are reported below.

Single Shot Results

The boundary layer structure in the Mach 8 facility has been observed using enhanced Rayleigh scattering from submicron-scale CO_2 particles, constituting a CO_2 "fog" in the core of the flow. This condensation is controlled by the addition of CO_2 gas into the air upstream of the wind tunnel plenum. The CO_2 fog generates a high contrast between the cold core of the flow and the hot boundary layers, so that outer layer boundary layer structure can easily be observed. This CO_2 fog is necessary since the Rayleigh scattering from the low density air itself is not sufficiently strong to generate single pulse images. Furthermore, the CO_2 fog highlights the temperature gradient much more effectively than does a measurement of the density profile. Studies have been completed to determine what the effect of the CO_2 is on the flow itself. CO_2 condensation adds heat in the nozzle and fast condensation, as well as fast vaporization, implies that the Rayleigh images do, indeed, correspond to a temperature profile. Careful measurements indicate that the CO_2-induced effects on the flow are small. For example, the Mach number is decreased by 1.6% for 1% CO_2 seeding. Changes in the nozzle wall pressure profile are shown in Fig. 5 as a function of normalized nozzle length, and indicate that, with 1% CO_2 seeding, condensation occurs 25% down the nozzle; whereas at 0.2%, condensation occurs 40% down the nozzle. Using this seeding and a double-pulsed Nd:YAG laser, planform views of the turbulent boundary layer structure in the Mach 8 flow above a flat plate have been taken (Fig. 6). The fact that these two images were taken with such a long delay and with separate cameras makes it difficult to evaluate the dynamics of the turbulence. The pulse-burst laser, however, is capable of taking similar images at up to a 1 MHz repetition rate, and uses a single camera.

The CO_2-enhanced Filtered Rayleigh Scattering was used to observe transition on two sharp-nosed elliptic cones--a 2:1 elliptic cone at Reynolds numbers ranging from 0.65×10^6 to 2.1×10^6 (based on the freestream conditions and distance to the measuring station), and a 4:1 elliptic cone at Reynolds numbers between 0.74×10^6 and 3.3×10^6. Boundary layers ranging from fully laminar-to-late transitional in character were first imaged using single-shot, streamwise, and spanwise laser orientations. For these experiments the stagnation pressures were varied between 150 and 1,500 psi, with a stagnation temperature of up to 870 K. The 4:1 elliptic model measured 0.2416 meters with a 17.5 degree half-angle on the major axis, and the 2:1 model measured 0.1524 meters with a 13.8 degree half-angle on the major axis.

The first model was manufactured to match the computations of Huang, et al. (1995). The second model was actually the nose section of the 1.016 m cone which was used by Poggie and Kimmel (1998). A schematic diagram for the sheet orientation for streamwise imaging is shown in Fig. 7, and for spanwise imaging is shown in Fig. 8. Figures 9 and 10 show streamwise images on the 4:1 elliptic cone and the 2:1 elliptic cone, respectively. The character of the flow ranges from what appears to be fully laminar to late transitional in both cases. Figure 11 is a montage of single-shot, spanwise Filtered Rayleigh Scattering images taken 21.5 cm from the nose along the 4:1 elliptic cone while varying the unit Reynolds number. In the spanwise images, the flow is moving out of the page, and the bright white line spanning the right-side of each frame is a result of residual unfiltered laser scatter from the model surface.

The streamwise images appear to show the existence of traveling wave instabilities on both the 4:1 and 2:1 elliptic cone models, and the spanwise images show structures which are not apparent in the streamwise direction. For example, spanwise roll-ups appeared near the centerline, which suggests the role of an inviscid instability. The centerline bulge at low Reynolds number is a result of the influx of low momentum fluid from the high pressure leading edge to the low pressure centerline of the model. At intermediate Reynolds numbers, spanwise vortices become apparent, and, at the highest Reynolds number, there are a wide range of scales and freestream fluid is entrained deeply into the boundary layer. The organized nature of the disturbances in frames 2A and 2B seems to suggest a mechanism by which the laminar centerline bulge breaks down.

The flow visualization appears to indicate that transition begins close to the centerline with the emergence of spanwise vortices on either side of the centerline bulge. In an apparent contradiction with previous understanding, these images indicate that the earliest occurrence of transition appears in a region near the centerline, where cross-flow velocities should be very low, as opposed to off-axis in regions of high cross-flow velocities. Also, the structures roll-up with the sign of their vorticity oriented downstream, which is somewhat unexpected. Questions arise as to the role of the traveling waves seen in the streamwise visualizations, and how they affect the behavior of the spanwise mechanisms.

Simultaneous Imaging Results

Figure 12 is a montage of three pairs of simultaneous images taken of the boundary layer in the early stages of transition. The dashed line in the planform images represents the position of the spanwise sheet, while the dashed line in the spanwise image represents the position of the planform sheet. For this series, the planform sheet is placed at a distance 4 mm from the centerline surface of the model. The most striking feature in frames 12a and 12b is the appearance of a heart-shaped structure in the planform images. In looking at the corresponding spanwise images, it is clear that the middle bulge is actually the tail end of the heart-shaped structure. The two "side bulges" show up in the planform view as long thin structures which are aligned at almost 45 degrees from the flow axis.

In frame 12c, the spanwise sheet cuts through the front end of the distorted heart-shaped structure. The spanwise image shows that the centerline bulge seems to have broken into two large bulges. The small scale vortical structures which are attached to this "double-bulge" in the spanwise image again show up as elongated structures in the planform image which are aligned roughly 45 degrees to the flow axis.

These images help to illuminate the behavior observed in the spanwise images shown in Figure 11. From the planform images, it appears that the centerline bulge is actually highly three-dimensional. When sliced through the upstream edge, images similar to Figure 11c are produced. When the spanwise sheet cuts through the middle of the heart, images similar to 11a or 11b are produced where a single bulge is present with smaller scales developing off-axis. Finally, when images are taken of the downstream edge of the planform heart, the smaller scales have grown to sizes which are equivalent to the original centerline bulge, and it appears as though three bulges exist (Figures 11d, 12a, 12b).

The images in Figures 13 and 14 are taken with the planform sheet positioned 3.5 and 3.0 mm from the surface, respectively. Again, the image pairs have been chosen which capture the different stages of the planform heart-shaped structures. For the planform images taken towards the interior of the boundary layer, the extent of the small vortical structures is shown. From Figure 14a, it is apparent that the small-scale structures imaged in the spanwise view actually extend far upstream. In fact, what appeared to be two separate structures may be one continuous loop which wraps around the upstream edge of the heart-shaped structure.

The planform images are an important piece in determining the physical mechanism behind these structures which appear in the early stages of transition. Since our use of the Filtered Rayleigh Scattering technique depends on condensed CO_2 to enhance the signal, it is possible to make assumptions about the flow direction in the planform images. The bright regions of condensed CO_2 are assumed to possess downward velocity, since this would represent freestream fluid which is being entrained in the boundary layer but which has not yet been close enough to the wall to sublimate the CO_2. Conversely, the dark regions represent fluid that has already come in close contact with the wall, and is now moving away from the surface.

Megahertz "Movie" Results

The pulse-burst laser system allows us to image consecutive frames to analyze the development of these structures. A series of flow visualizations were performed on both 4:1 and 2:1 sharp-nosed elliptic cones at Mach 8. Boundary layers ranging from fully laminar to late-transitional in character were imaged with streamwise, spanwise, and planform laser sheet orientations. A selection of movies in Quicktime format is available for viewing on the web sites: http://www.princeton.edu/~gasdyn/Research/EllCone_FRS.html, and http://www.princeton.edu/~milesgrp/BBL.html.

The "movies" reveal a rather slow development of the flow structure. This result was used to produce quasi-volumetric image sets of the centerline region, where the time between successive spanwise images were transformed to space using the freestream velocity as the convection velocity. Some representative results are shown in Figures 15 and 16. The images are consistent with the presence of hairpin structures characteristic of the early stages of subsonic turbulent spot formation. At low Reynolds number, the unstable region on the cone was confined to the bulge of the centerline boundary layer and the lateral evolution of these hairpin structures was minimal (Figure 15). Images of the off-axis regions at higher

Reynolds numbers (Figure 16) reveal mechanisms that appeared qualitatively similar to the breakdown of crossflow vortices observed on spinning axisymmetric bodies at subsonic speeds.

Publications Acknowledging the Grant:

Erbland, P.J., Etz, M.R., Huntley, M., Smits, A.J. and Miles, R.B., "Imaging the Evolution of Turbulent Structures in a Hypersonic Boundary Layer," AIAA paper #98-2510, 20th AIAA Advanced Measurement and Ground Testing Conference, Albuquerque, NM, June 15-June 18, 1998.

P.J. Erbland, R. Murray, M.R. Etz, M. Huntley, and R.B. Miles, "Imaging the Evolution of Turbulent Structures in a Hypersonic Boundary Layer," Paper #AIAA-99-0769, 37th AIAA Aerospace Sciences Meeting and Exhibit, Jan. 11-14, 1999, Reno, NV.

Huntley, M. and Smits, A.J. "Transition Studies on an Elliptic Cone in Mach 8 Flow Using Filtered Rayleigh Scattering," European Journal of Mechanics B–Fluids, to appear August, 2000.

Huntley, M. and Smits, A.J. "Transition Studies on Elliptic Cones in Mach 8 Flow Using Filtered Rayleigh Scattering," First International Symposium on Turbulence and Shear Flow Phenomena, Sept. 12-15, 1999, Santa Barbara, CA.

Huntley, M., Erbland, P., Kimmel, R., Poggie, J. and Smits, A.J., "Transition Studies on Elliptic Cones in Mach 8 Using Filtered Rayleigh Scattering," Paper #Ia4, 50th Meeting of the American Physical Society Division of Fluid Dynamics, San Francisco, CA, November 23-25, 1997.

Huntley, M. and Smits, A.J., "Transition Studies on an Elliptic Cone in Mach 8 Flow Using Filtered Rayleigh Scattering," Paper #AF3, 51st Meeting of the American Physical Society Division of Fluid Dynamics, Philadelphia, PA, November 22-24, 1998.
of Fluid Dynamics, New Orleans, LA, November 21-23, 1999.

Huntley, M. and Smits, A.J., "MHz Rate Imaging of Boundary Layer Transition on Elliptic Cones at Mach 8," Paper #KL3, 52nd Meeting of the American Physical Society Division of Fluid Dynamics, New Orleans, LA, November 21-23, 1999.

R.B. Miles, "Planar Laser Imaging," Chapter 5 in "Flow Visualization: Techniques and Examples" ed. by A.J. Smits and T.T. Lim, Imperial College Press, 2000.

P. Wu, W.R. Lempert, and R.B. Miles, "MHz Pulse-Burst Laser System and Visualization of Shock Wave/Boundary Layer Interaction," *AIAA Journal,* (to be published) Vol. 38, No. 1, January 2000.

References

Bogdanoff, D.W., "Compressibility Effects in Turbulent Shear Layers," AIAA Journal, Vol. 21, pp. 926-927, 1983.

Bradshaw, P. "Effects of Streamline Curvature on Turbulent Flow," AGARDograph No. 196 (1973).

Bradshaw, P. "Review: Complex Turbulent Flows," J. Fluids Engin., Vol. 97, p. 146 (1975).

Bradshaw, P. "Effects of Extra Strain Rates - Review," Zoran Zaric Memorial Conference on Near-Wall Turbulence, Hemisphere (1988).

Castro, I.P. and Bradshaw, P., "The Turbulence Structure of a Highly Curved Mixing Layer," Journal of Fluid Mechanics, Vol. 73, pp. 265-304 (1976).

Cheng, T.S., Wehrmeyer, J.A., and Pitz, R.W., (1992), Comb. and Flame 91, 323.

Cogne, S., Forkey, J., Miles, R.B. and Smits, A.J., "The Evolution of Large-Scale Structures in a Supersonic Turbulent Boundary Layer," Proceedings Symposium on Transitional and Turbulent Compressible Flows, ASME Fluids Engineering Conference, Washington, D.C., June 20-24, 1993.

Delo, C., and Smits, A.J., "Visualization of the Three- Dimensional, Time-Evolving Scalar Concentration Field in a Low Reynolds Number Turbulent Boundary Layer.", Proc. Second International Symposium on Near-Wall Turbulent Flows, R.M.C. So, C.G. Speziale and B.E. Launder, Eds., Elsevier Science Publishers, 1993.

Delo, C., Poggie, J. and Smits, A.J., "A System for Imaging and Displaying Three-Dimensional, Time-Evolving Passive Scalar Concentration Fields in Fluid Flow", Princeton University, Dept. of Mechanical and Aerospace Engineering, Report #1992, 1994.

Forkey, J., Cogne, S., Smits, A.J., Lempert, W. and Miles, R.B. 1993, "Time-sequenced and spectrally filtered Rayleigh imaging of shock wave and boundary layer structure for inlet characterization," AIAA/SAE/ASME/ASEE Joint Propulsion Conference, Monterey CA, June 28 - 30, 1993.

Gillis, J.C. and Johnston, J.P., "Turbulent Boundary Layer Flow and Structure on a Concave Wall and Its Redevelopment on a Flat Wall, Journal of Fluid Mechanics, Vol. 135 pp. 123-153 (1983).

Huang, S.L., Stuckert, G.K. and Herbert, T. "Cross Flow Instability of the Supersonic Flow Over a 4:1 Elliptic Cone. Dynaflow, Inc. Report, 1995.

Konrad, W.A., (1993), PhD Thesis, Dept of Mech and Aerospace Engrg, Princeton University.

Konrad, W., Smits, A.J. and Knight, D., (1994) Expt'l Thermal and Fluid Science, Vol. 9, No. 2, p. 156

Lempert, W.R., Wu, P-F., and Miles, R.B (1997), AIAA-97-0500, 35th Aerospace Sciences Meeting, Reno, NV, Jan 6-10, 1997.

McDaniel, J.C., Hiller, B., and Hanson, R.K. (1983), Opt. Lett. 8, 51.

Miles, R. and Lempert, W., (1990) Appl. Phys. B51, 1.

Miles, R., J.N. Forkey, and Lempert, W.R. (1992), AIAA-92-3894, 17th Aerospace Ground Test Conference, Nashville, TN, July 6-8, 1992.

Miles, R. and W. Lempert, "Two-Dimensional Measurement of Density, Velocity, and Temperature of Turbulent Air Flows from UV Rayleigh Scattering," Applied Physics B B51, July 1990, p. 1.

Miles, R., W.R. Lempert, B. Zhang, J. Forkey, and I. Glesk, "Rayleigh Imaging and Flow Tagging in Ground Test Facilities," Proceedings 14th International Congress on Instrumentation in Aerospace Simulation Facilities, IEEE Publication 91 CH3028-8, p. 255, IEEE Aerospace and Electronic Systems Society, Oct. 27-31, 1991.

Miles, R., J.N. Forkey, and W.R. Lempert, "Filtered Rayleigh Scattering Measurements in Supersonic/Hypersonic Facilities," Paper #AIAA-92-3894, AIAA 17th Aerospace Ground Testing Conference, Nashville, TN, July 6-8, 1992.

Morkovin, M. V., "Effects of compressibility on turbulent flows," Int. Symp. on the Mechanics of Turbulence 367. C.N.R.S., Paris, 1962.

Nau, T.A. "A Quantitative Evaluation of Rayleigh Scattering Techniques for Density Measurements in Supersonic Turbulent Boundary Layers", MSE Thesis, Princeton University, 1994.

Papamoschou, D. and Roshko, A., "The Compressible Turbulent Mixing Layer: An Experimental Study," Journal of Fluid Mechanics, Vol. 197, pp. 453-477, 1988.

Poggie, J. and Kimmel, R.L. "Traveling Instabilities in Elliptic Cone Boundary Layer Transition at Mach 8. AIAA 36th Aerospace Sciences Meeting, Reno, NV. Jan. 1998.

Russell, G. and Miles, R., "Display and Perception of Three-Dimensional Spacing-Filling Data," Applied Optics 26, March 1987, page 973.

Seitzman, J.M., Kyachoff, G., and Hanson, R.K., (1985), Opt. Lett. 10, 439.

Settles, G.S. and Dodson, L.J., (1992), NASA CR 177577

Smith, M., A. Smits, and R. Miles, "Compressible Boundary Layer Density Cross Sections by UV Rayleigh Scattering," Optics Letters 14, 1989.

Smith, M. W. and Smits, A. J., "Cinematic visualization of coherent density structures in a supersonic turbulent boundary layer," AIAA Paper 88- 500, 1988.

Smits, A.J. "The Control of Turbulent Boundary Layers by the Application of Extra Strain Rates," AIAA Paper 85-0538, AIAA Shear Flow Control Conference, Boulder, Colorado (1985).

Smits, A. J. and Dussauge, J.P., *"Turbulent Shear Layers in Compressible Flow,"* 1996, Springer-Verlag.

Smits, A.J., Young, S.T.B. and Bradshaw, P., "The Effect of Short Regions of High Surface Curvature on Turbulent Boundary Layers", Journal of Fluid Mechanics, Vol.94, pp.209-242 (1979).

Smits, A.J. and Wood, D.H., "The Response of Turbulent Boundary Layers to Sudden Perturbations", Annual Review of Fluid Mechanics, Vol.17, pp.321-58 (1985).

Spina, E.F., Donovan, J.F. and Smits, A.J. "On the Structure of High- Reynolds- Number Supersonic Turbulent Boundary Layers," Journal of Fluid Mechanics, Vol. 222, pp. 293-327 (1991).

Spina, E.F., Robinson, S.K. and Smits, A.J. "The Physics of Supersonic Turbulent Boundary Layers." To appear Annual Review of Fluid Mechanics, Vol. 26 (1994).

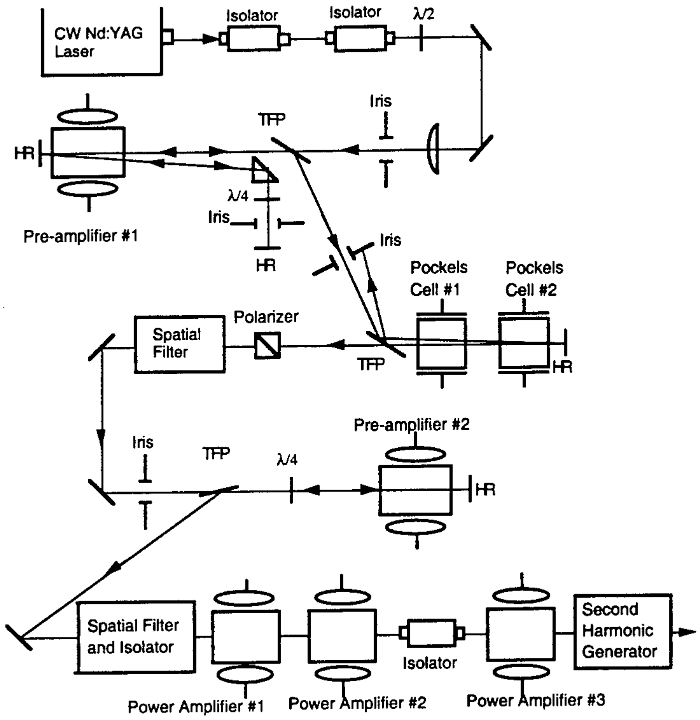

Figure 1: Schematic Diagram of Pulse Burst Laser

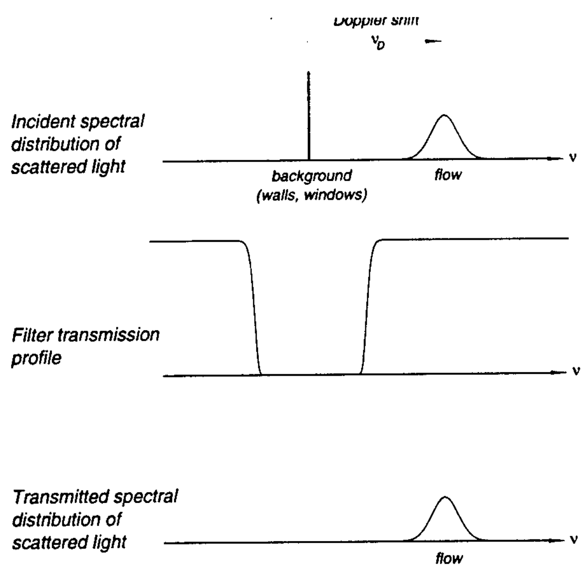

Figure 2: Basic Filtered Rayleigh Scattering concept

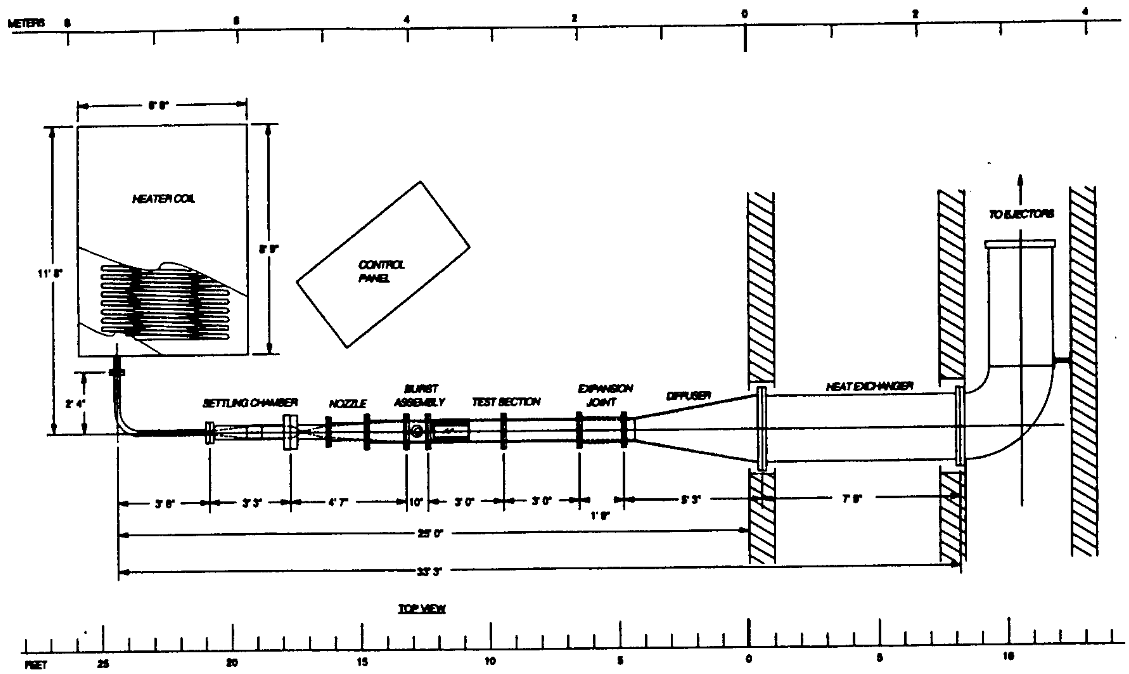

Figure 3: Diagram of Princeton University Mach 8 Facility

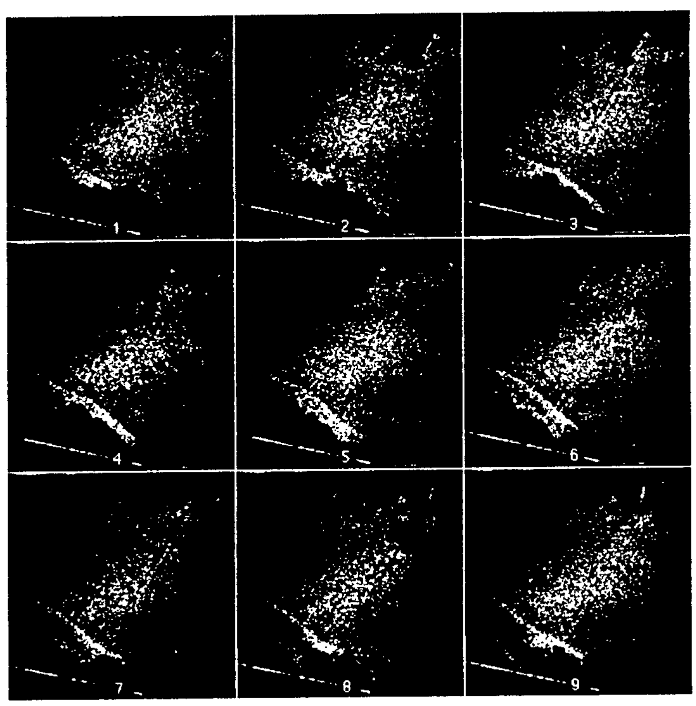

Figure 4: Time Sequence of 9 Images of Mach 2.5 flow over 14° wedge.
Flow is from right to left. 2 microseconds between images

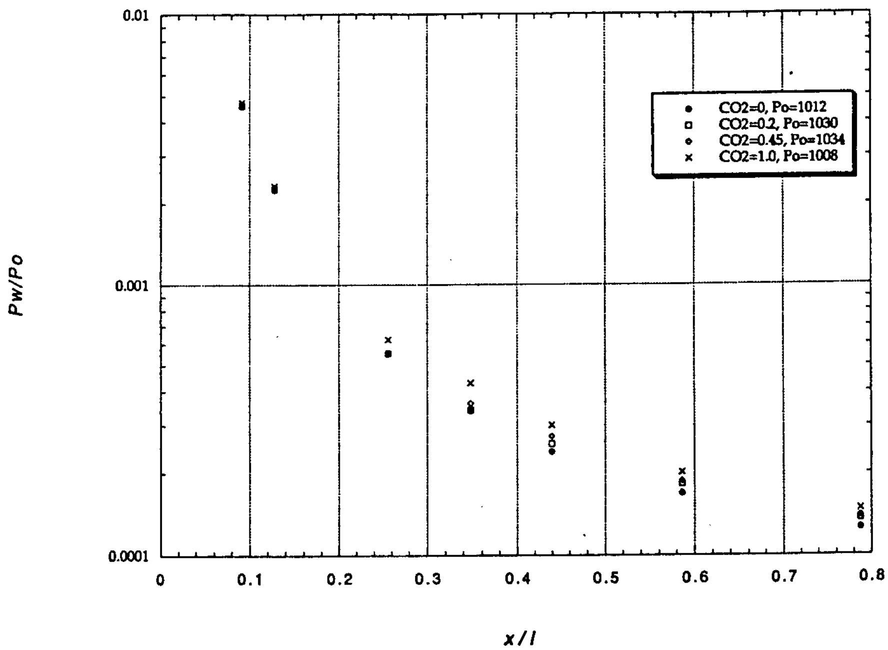

Figure 5. Nozzle pressure distribution. Pressure rise due to CO_2 seeding. Data averaged over multiple runs.

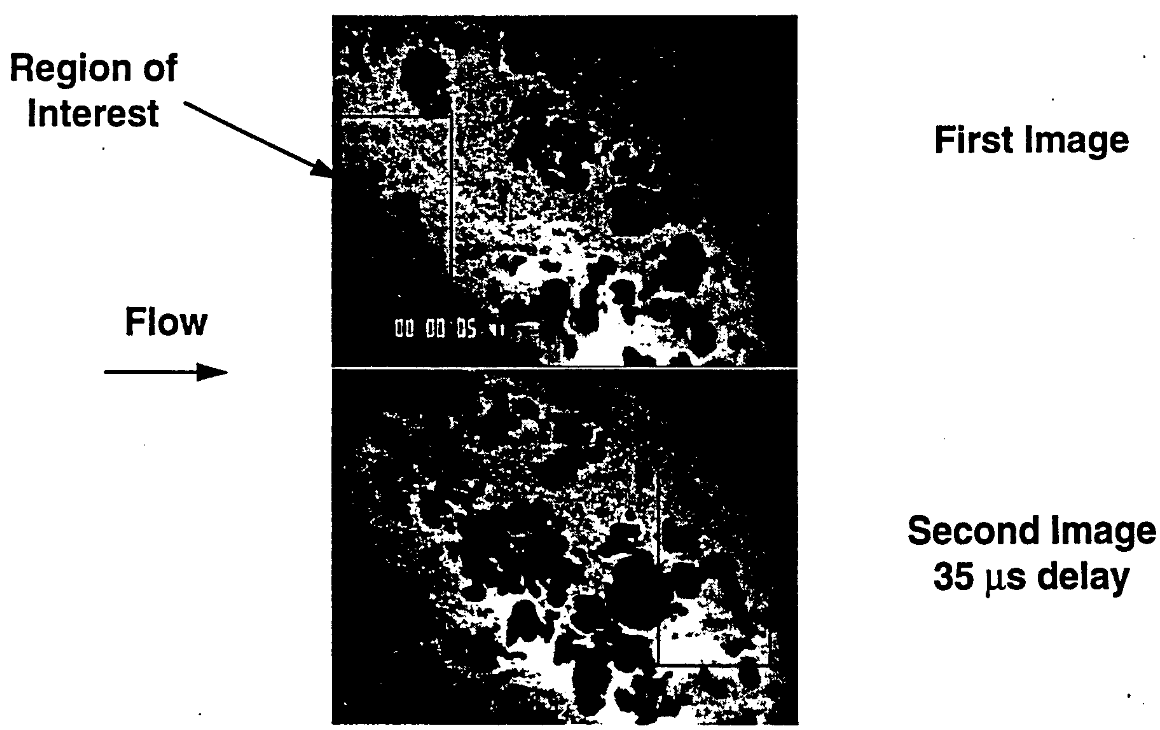

Figure 6. CO_2 enhanced Filtered Rayleigh Scattering of Mach 8 flat plate turbulent boundary layer. Planform view. Field of view: 57 x 43 mm, 400 mm aft of leading edge, $Re_\theta = 3500$.

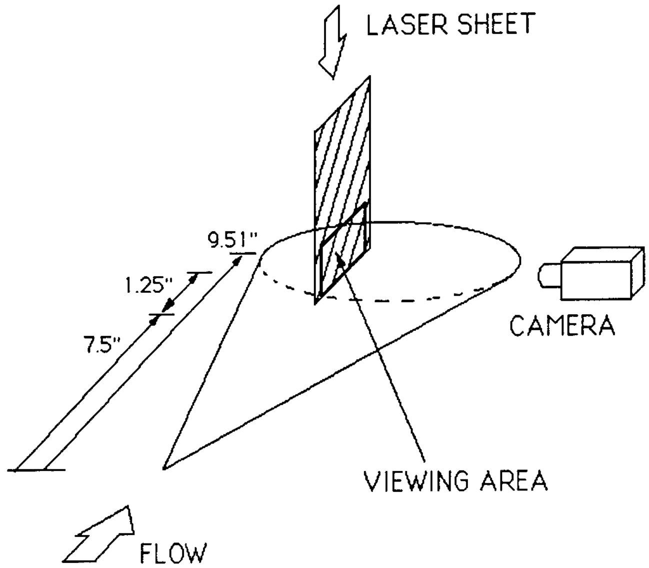

Figure 7. Schematic diagram of sheet orientation for streamwise imaging. Dimensions are for tests on the 4:1 elliptic cone. Field-of-view was approximately 2.5 cm x 2 cm, with long dimension in the streamwise direction.

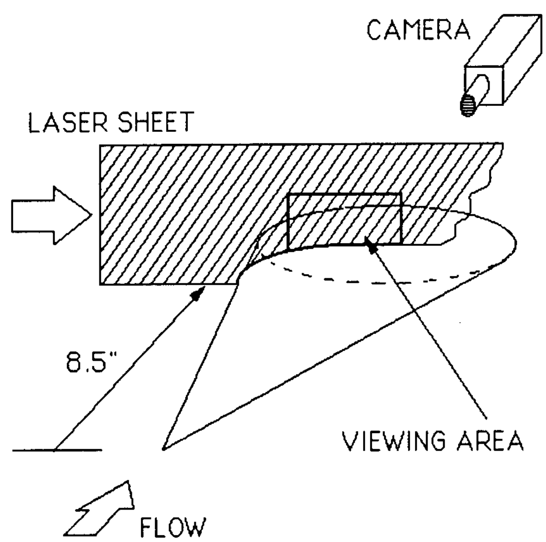

Figure 8. Schematic diagram of sheet orientation for spanwise imaging. Dimensions are for tests on the 4:1 elliptic cone. Field-of-view was approximately 3.5 x 2.5 cm with long dimension in the spanwise direction.

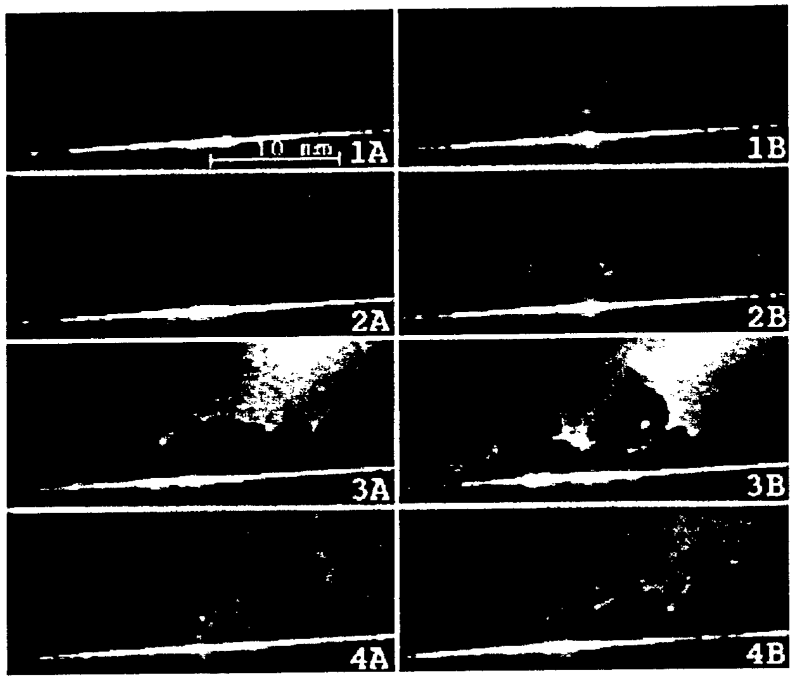

Figure 9. Streamwise Filtered Rayleigh Scattering on 4:1 elliptic cone. Flow is from left-to-right. 1A,1B: $Re_x=1.1x10^6$. 2A,2B: $Re_x=1.7x10^6$. 3A,3B: $Re_x=2.3x10^6$. 4A,4B: $Re_x=2.8x10^6$.

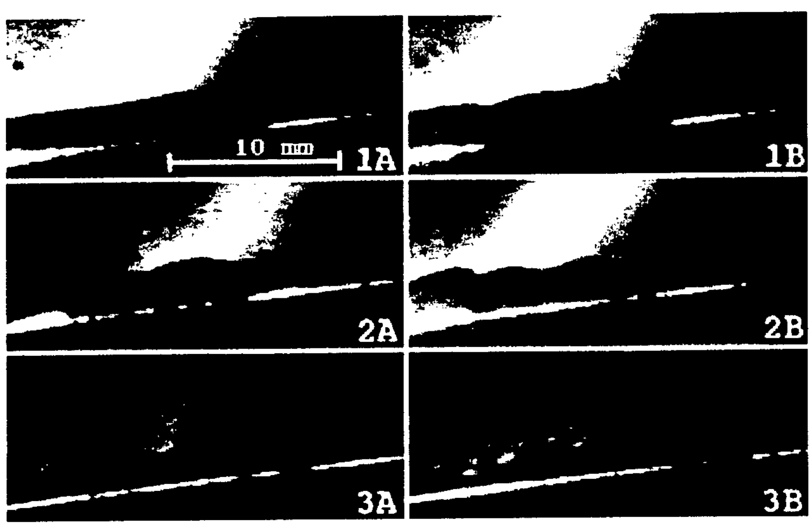

Figure 10. Streamwise Filtered Ralyeigh Scattering on 2:1 elliptic cone. Flow is from left-to-right. 1A,1B: $Re_x=1.1x10^6$. 2A,2B: $Re_x=1.4x10^6$. 3A,3B: $Re_x=1.7x10^6$.

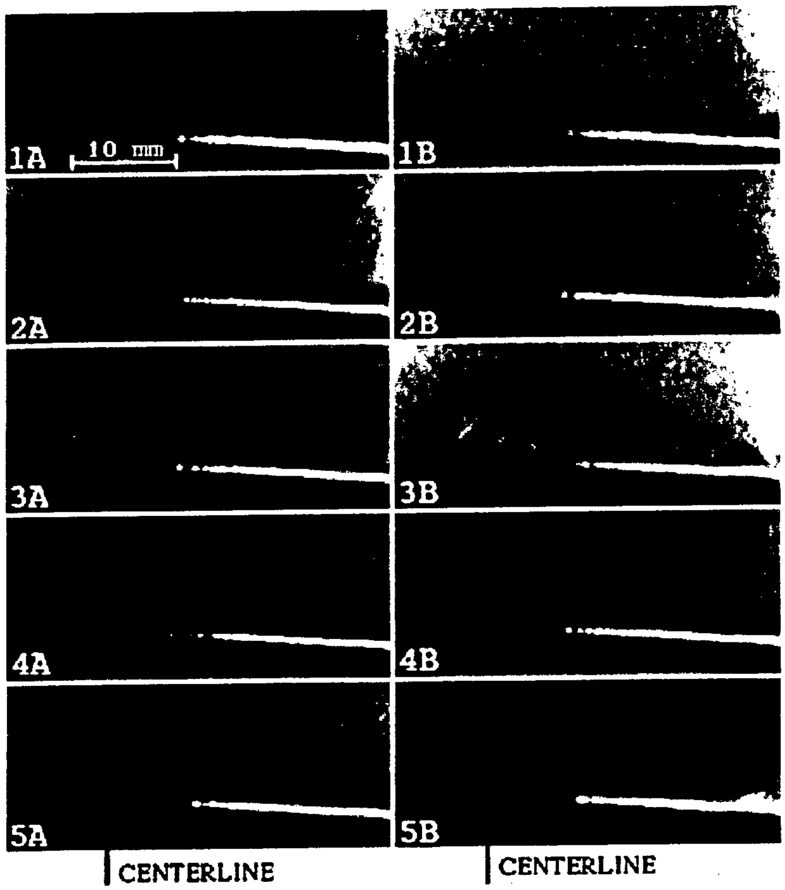

Figure 11. Spanwise Filtered Rayleigh Scattering on 4:1 elliptic cone. Flow is moving out of the image plane. 1A,1B: Re_x=0.7x10^6. 2A,2B: Re_x=1.2x10^6. 3A,3B: Re_x=1.8x10^6. 4A,4B: Re_x=2.4x10^6. 5A,5B: Re=3.0x10^6.

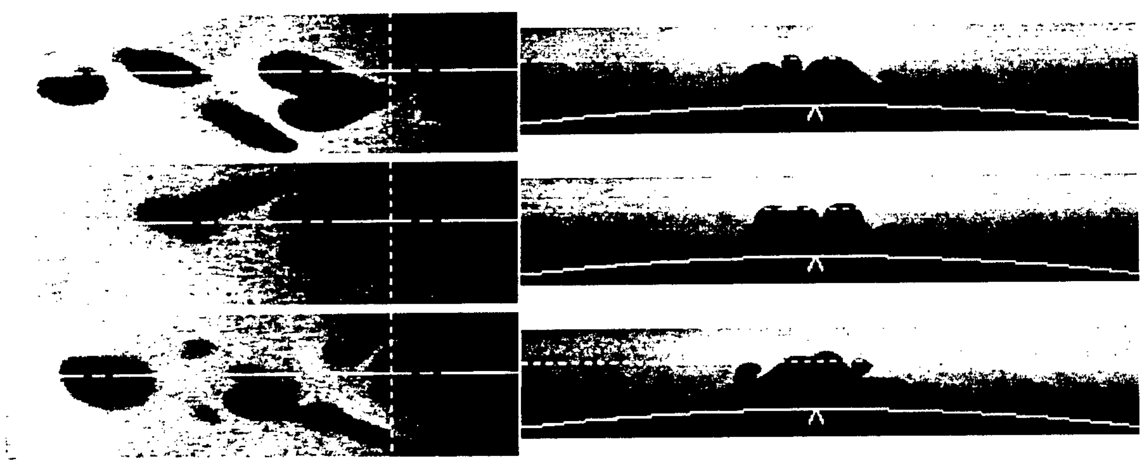

Figure 12. Simultaneous images of planform (left) and spanwise (right) planes. Dashed line represents the intersection of the two planes. Flow is from left to right in planform and out of the page for the spanwise image. Planform sheet is positioned 4.0mm from the model surface.

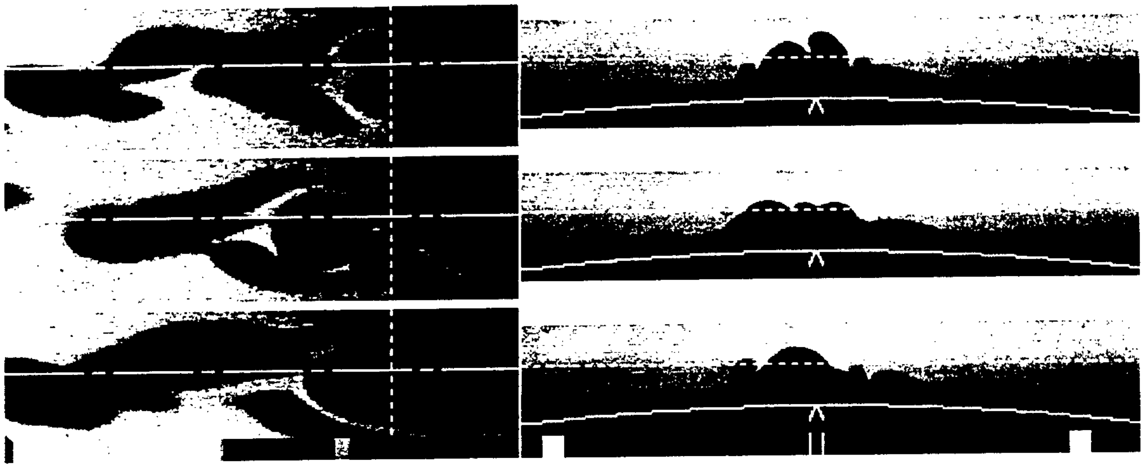

Figure 13. Simultaneous images of planform (left) and spanwise (right) planes. Dashed line represents the intersection of the two planes. Flow is from left to right in planform and out of the page for the spanwise image. Planform sheet is positioned 3.5mm from the model surface.

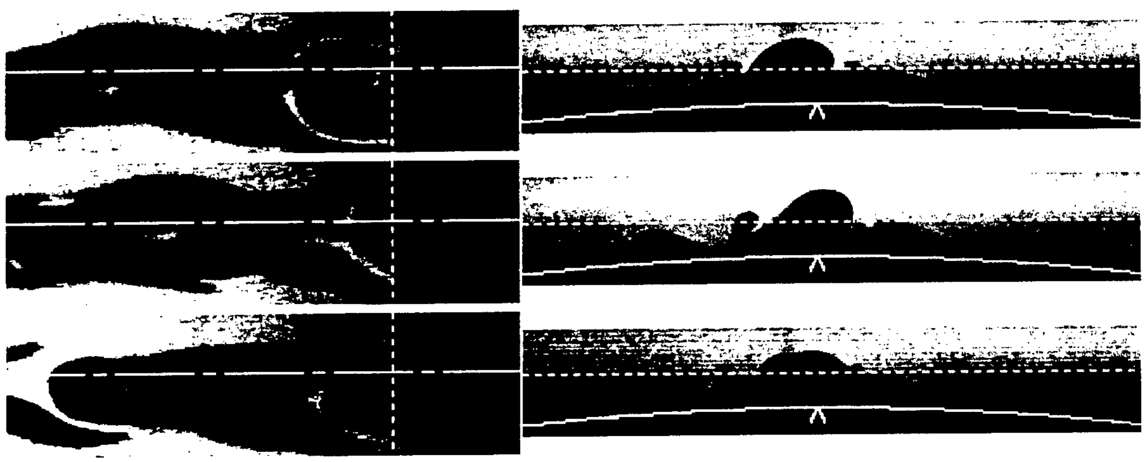

Figure 14. Simultaneous images of planform (left) and spanwise (right) planes. Dashed line represents the intersection of the two planes. Flow is from left to right in planform and out of the page for the spanwise image. Planform sheet is positioned 3.0mm from the model surface.

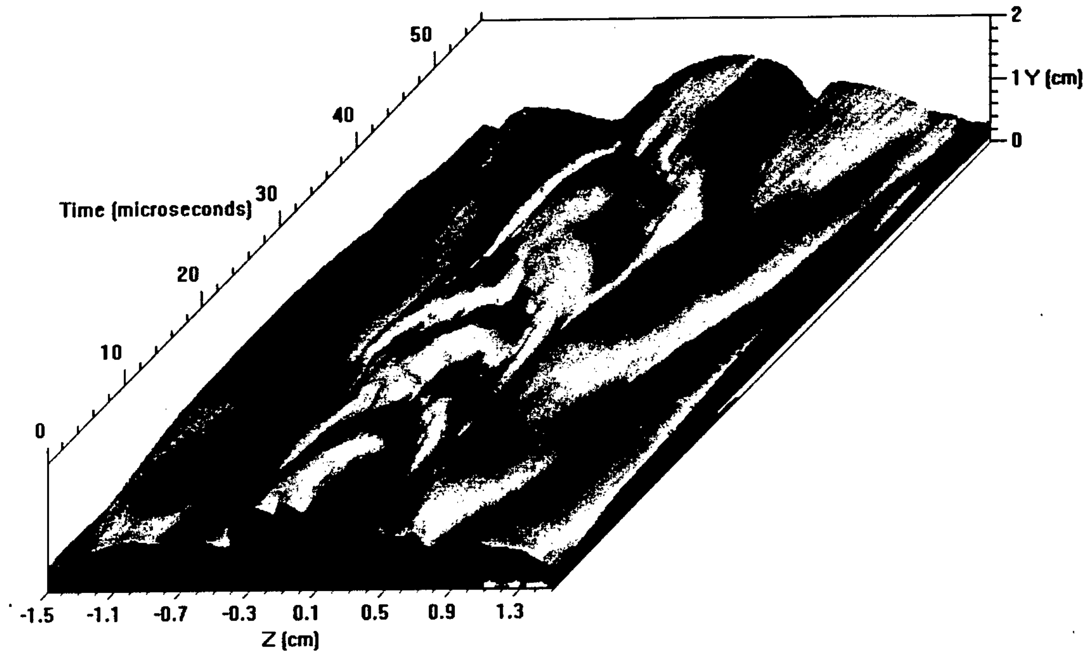

Figure 15: Centerline structure, 4:1 ellipsoid, quasi-volumetric view derived from 28 images at 500 KHz. $Re_x = 1.57 \times 10^6$. Flow toward lower left corner of image.

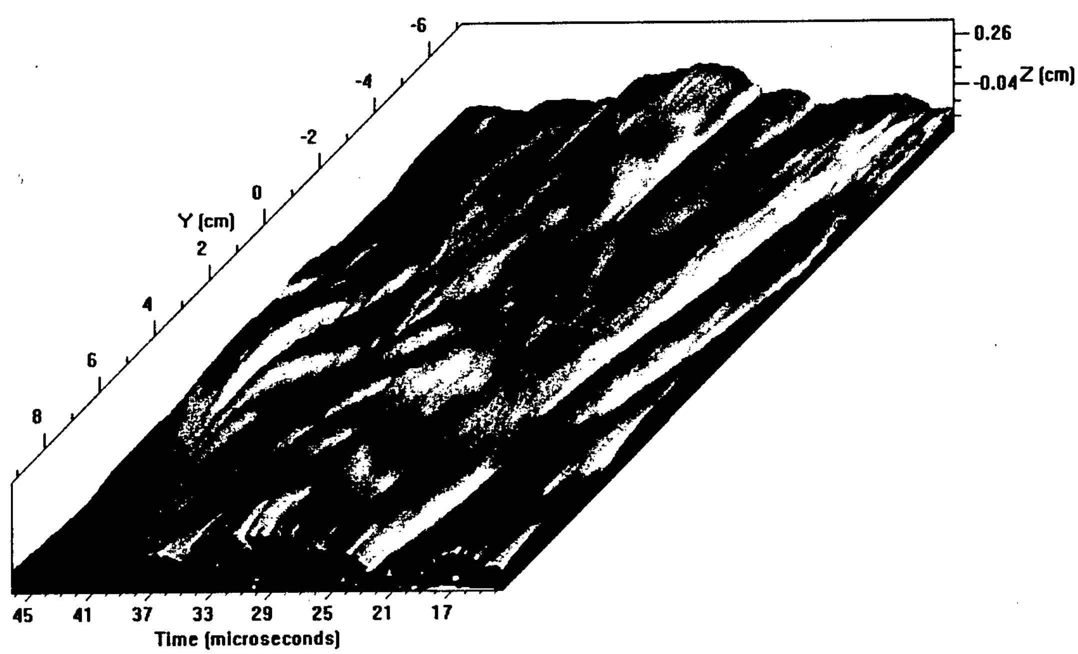

Figure 16: Off-axis structure, 4:1 ellipsoid, quasi-volumetric view derived from 28 images at 500 KHz. $Re_x = 1.57 \times 10^6$. Flow toward lower left corner of image.